

Deformation of rotational structures in ^{73}Kr and ^{74}Rb : Probing the additivity principle at triaxial shapes

F. Johnston-Theasby,¹ A. V. Afanasjev,^{2,3} C. Andreoiu,⁴ R. A. E. Austin,⁵ M. P. Carpenter,⁶ D. Dashdorj,⁷ S. J. Freeman,⁸ P. E. Garrett,^{4,9} J. Greene,⁶ A. Gorgen,¹⁰ D. G. Jenkins,¹ P. Joshi,¹ A. O. Macchiavelli,¹¹ F. Moore,⁶ G. Mukherjee,^{6,*} W. Reviol,¹² D. Sarantites,¹² D. Seweryniak,⁶ M. B. Smith,⁹ C. E. Svensson,⁴ J. J. Valiente-Dobon,¹³ R. Wadsworth,¹ and D. Ward¹¹

¹*Department of Physics, University of York, Heslington, York YO10 5DD, United Kingdom*

²*Department of Physics and Astronomy, Mississippi State University, Mississippi 39762, USA*

³*Laboratory of Radiation Physics, Institute of Solid State Physics, University of Latvia, LV 2169 Salaspils, Miera str. 31, Latvia*

⁴*Department of Physics, University of Guelph, Guelph, Ontario N1G 2W1, Canada*

⁵*Department of Physics and Astronomy, McMaster University, Hamilton, Ontario L8S 4K1, Canada*

⁶*Physics Division, Argonne National Laboratory, Argonne, Illinois 60439, USA*

⁷*North Carolina State University, Raleigh, North Carolina 27695, USA*

⁸*Department of Physics and Astronomy, University of Manchester, Manchester M15 9PL, United Kingdom*

⁹*TRIUMF, 4004 Wesbrook Mall, Vancouver, British Columbia, V6T 2A3, Canada*

¹⁰*CEA Saclay, IRFU/Service de Physique Nucleaire, F-91191 Gif-sur-Yvette, France*

¹¹*Lawrence Berkeley National Laboratory, Berkeley, California 94720, USA*

¹²*Department of Chemistry, Washington University, St. Louis, Missouri 63130, USA*

¹³*INFN, Laboratori Nazionali di Legnaro, I-35020, Legnaro, Italy*

(Received 14 May 2008; published 18 September 2008)

Lifetimes have been deduced in the intermediate/high-spin range for the three known rotational bands in ^{73}Kr and the $T = 0$ band in ^{74}Rb using the residual Doppler shift method. This has enabled relative transition quadrupole moments to be studied for the first time in triaxial nuclei as a function of spin. The data suggest that the additivity principle for transition quadrupole moments is violated, a result that is in disagreement with predictions from cranked Nilsson-Strutinsky and cranked relativistic mean-field theory calculations. The reasons for the discrepancy are not understood but may indicate that important correlations are missing from the models.

DOI: [10.1103/PhysRevC.78.034312](https://doi.org/10.1103/PhysRevC.78.034312)

PACS number(s): 23.20.Lv, 21.10.Re, 21.60.Ev, 27.50.+e

I. INTRODUCTION

Studies of nuclei in the $N \sim Z$ mass 70 region are of great interest because of the rich variety of physical phenomena that they display at both low and high spin, with shape changes as a function of spin and shape coexistence being just two recently studied examples [1,2]. It is well known from Nilsson and Woods-Saxon calculations that large prolate and oblate shell gaps, ~ 2 MeV, exist for both neutrons and protons at $\beta_2 \sim +0.4$ for particle numbers 38, 40 and at $\beta_2 \sim -0.3$ for particle numbers 34, 36 [3]. This can lead to large shape changes in nuclei in this region with the removal or addition of only one or two nucleons. For example, ^{72}Kr is expected to have an oblate ground state [4,5] with a low-lying prolate isomer [6], whereas in ^{74}Kr the situation seems to be reversed, with a prolate ground state [7] and a low-lying oblate isomer [2,8,9]. Another phenomenon of great interest in this region is proton-neutron pairing. Although the role of the isovector proton-neutron pairing is well established in the $N \approx Z$ nuclei, so far there are no definitive indications of the presence of the isoscalar component of this pairing mode (see Ref. [10] and references therein). ^{74}Kr also provides the first experimental evidence for the newly observed phenomenon

of nontermination of rotational bands at $I = I_{\text{max}}$: here the bands do not lose their collectivity and thus do not terminate in a noncollective single-particle state at $I = I_{\text{max}}$ [11]. This feature is in complete contrast to what is observed for smooth terminating bands in, for example, ^{62}Zn [12] and ^{109}Sb [13].

Detailed studies require lifetime measurements, because such data will yield vital information on the influence that single particle(s) have on the shape of the nucleus and its evolution with spin, as well as providing important data to aid the interpretation of the structure of the bands and their properties. A further interesting feature is that if lifetime measurements can be obtained for several bands in neighboring nuclei from a single experiment, it will be possible to test whether the additivity principle for quadrupole moments is valid for triaxial or γ -soft nuclei in this mass region. This latter feature is a major goal of the current work.

The basic idea behind the principle of additivity is quite simple: the value of the physical observable $O(k)$ of the k th configuration in question, with respect to the value of the same observable for the "core" configuration, is defined by the sum of effective contributions of particle and hole states by which the "core" configuration differs from the k th configuration [14–16]. The choice of "core" configuration is completely arbitrary. The additivity of single-particle quantities means that the polarizations due to different particles and/or holes are to a large extent independent of one another. The additivity principle for quadrupole moments has been confirmed so

*Present address: Variable Energy Cyclotron Centre, Kolkata 700064, India.

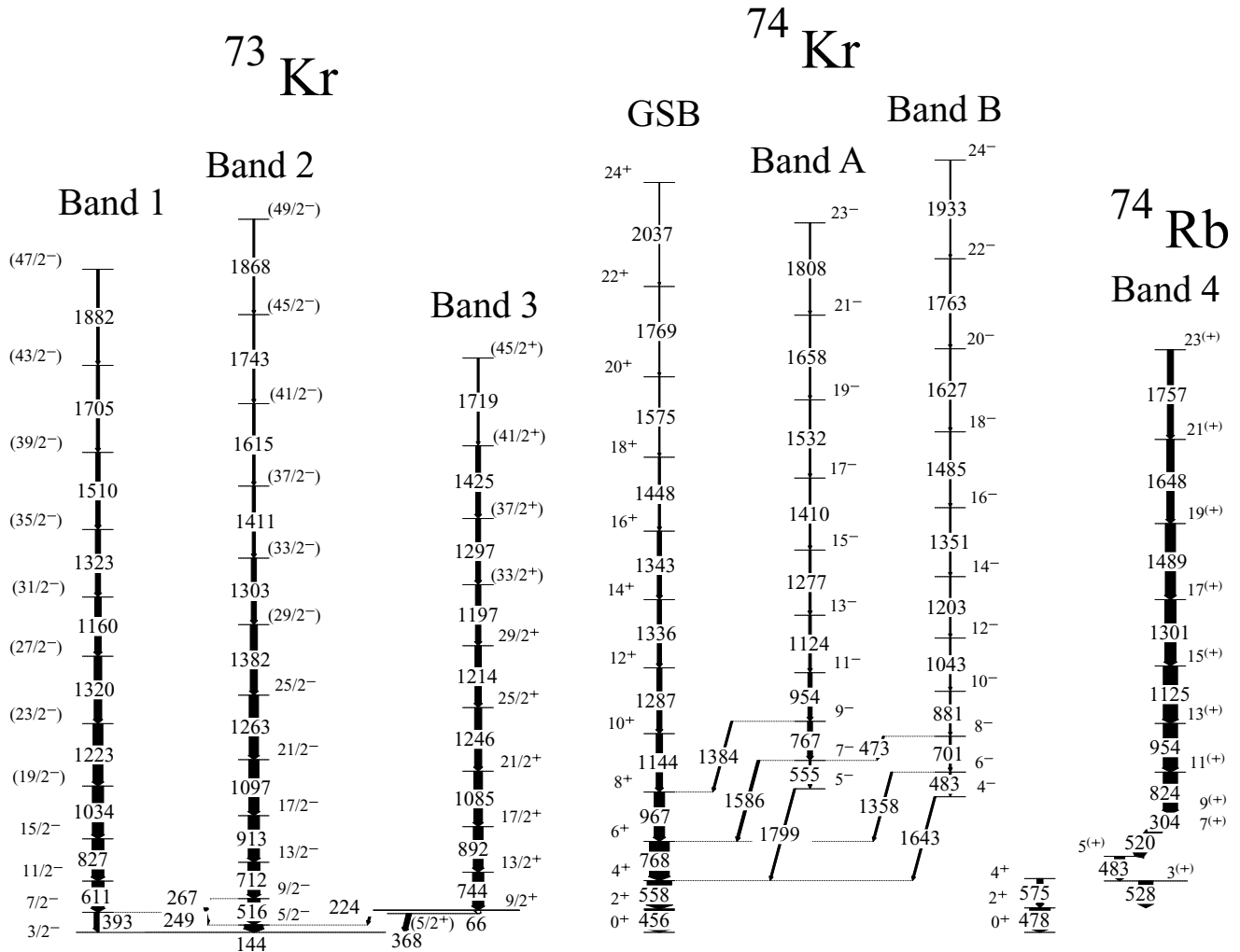


FIG. 1. Partial level schemes showing the bands of interest to the present study. The data were taken from Refs. [11,23,32], with a slight modification to the ^{74}Rb level scheme, which is discussed in Sec. III.

far only for the nuclei in the $A \sim 150$ [15,17–19] and $A \sim 130$ [20,21] mass regions of superdeformation, which are characterized by near-prolate deformation and negligible pairing between like particles. No studies of the validity of the principle of additivity have been reported for triaxial or γ -soft nuclei. The data for the nuclei $^{73,74}\text{Kr}$ and ^{74}Rb allow, for the first time, tests to be carried out on the validity of the additivity principle for transition quadrupole moments in rotational bands that are not axially prolate but are expected to possess some degree of γ deformation and be γ soft (see Ref. [10] (in particular, Figs. 2, 11, and 15) and references therein). For example, the cranked Nilsson-Strutinsky (CNS) calculations show that in the spin range $12-26\hbar$ the γ deformations of the ground-state band in ^{74}Kr , band 4 in ^{74}Rb , and bands 2 and 3 in ^{73}Kr change in the range $(1^\circ \rightarrow 9^\circ)$, $(-4^\circ \rightarrow 8^\circ)$, $(-11^\circ \rightarrow 16^\circ)$, and $(-2^\circ \rightarrow 17^\circ)$, respectively. Similar changes in γ deformation have been seen in other assigned configurations. These bands are observed to moderately high spin, where pairing may be expected to play a minor role, a further necessary condition for the additivity principle to hold [14,15].

In the current work, the lifetimes for all three known bands in ^{73}Kr have been measured in the intermediate spin range using thin targets and the residual Doppler shift technique [22]. They have also been determined for the strongest odd spin $T = 0$ band in ^{74}Rb (band 4 in Ref. [23]). The results for the two nuclei are compared with both the cranked Nilsson-Strutinsky (CNS) [24] and the cranked relativistic mean-field (CRMF) [25] model calculations. These data also provide the first opportunity to study the relative quadrupole moments between bands in the neighboring nuclei ^{74}Kr [11], ^{73}Kr , ^{74}Rb , because data for ^{74}Kr were measured in the same experiment. Figure 1 shows the relevant partial level schemes for all of the bands discussed in this manuscript.

II. EXPERIMENTAL METHOD AND ANALYSIS

The experiment was performed at the Argonne National Laboratory using the ATLAS accelerator to produce a ^{40}Ca beam at 165 MeV. This beam was used to bombard a $350\text{-}\mu\text{g}/\text{cm}^2$ ^{40}Ca target that was flashed on both sides with

150 $\mu\text{g}/\text{cm}^2$ of gold to prevent oxidation. The reaction channels of interest were $^{40}\text{Ca}(^{40}\text{Ca}, \alpha 2pn)^{73}\text{Kr}$ and $^{40}\text{Ca}(^{40}\text{Ca}, \alpha pn)^{74}\text{Rb}$. γ rays from the nuclei were detected using the Gammasphere array [26], which consisted of 99 Compton suppressed Ge detectors, and charged particle identification was performed using the Microball array [27]. An event was triggered on the condition of at least four of the high-performance germanium detectors firing in prompt coincidence. Information from the Microball array, consisting of the energies and direction of the detected charged particles and their identification, allowed for an offline event-by-event reconstruction of the momenta of the residual nuclei [28,29], thereby resulting in better energy resolution for the γ -ray peaks.

Events coinciding with the detection of an α particle and two protons were selected for the nucleus ^{73}Kr , whereas for ^{74}Rb events containing an α particle and a single proton were used. Further attempts to enhance the channels of interest using the total energy plane (TEP) method [30] did not significantly improve the quality of the spectra, hence an open TEP gate was used in the analysis to maximize statistics. The events were sorted into five $\gamma - \gamma$ matrices with γ rays detected at any angle on the y axis and events detected at angles of 35° , 52° , 90° , 128° , and 145° placed on the x axis, respectively. Some of these are effective angles and result from combining two rings of detectors in the Gammasphere array.

The lifetimes of the states in three bands in ^{73}Kr and one band in ^{74}Rb were deduced using the residual Doppler shift attenuation method [22]. This technique is useful for measuring the lifetimes of high-spin levels that decay while the nucleus is recoiling through the target. The events were Doppler corrected so that the energies of the γ rays emitted outside the target, i.e., γ transitions at the bottom of the rotational bands, lined up for all the Gammasphere rings. This defines the ratio $F_{\text{out}} = \beta_{\text{out}}/\beta_0$, where β_{out} is the average velocity of the recoiling nucleus outside the target and β_0 is the velocity that the residual nucleus was produced with at the center of the ^{40}Ca target. The γ transitions that were emitted within the target, i.e., those transitions at the middle/top of the rotational bands, present a ratio of $F(\tau) = \beta_\tau/\beta_0$, where β_τ changes for each transition as a result of the residual Doppler shift. By plotting the centroid energies of the Doppler-corrected γ transitions versus the cosine of the angles for the different Gammasphere rings one can obtain ΔF from the slope of this line, which then determines the final $F(\tau)$, because $F(\tau) = F_{\text{out}} + \Delta F$. Finally, $F(\tau)$ versus the spin of the state is plotted. These curves were subsequently fitted using a code that models the slowing down of the nucleus in the target and the thin Au backing layer to extract the best fit quadrupole moments of the states in each band (see Ref. [11] for details).

III. RESULTS

To produce the Doppler-shifted spectra it was necessary to gate on in-band transitions for each of the matrices. For band 1 in ^{73}Kr this was achieved by combining four single-gate spectra produced by gating on the 249-, 393-, 611-, and 1223-keV

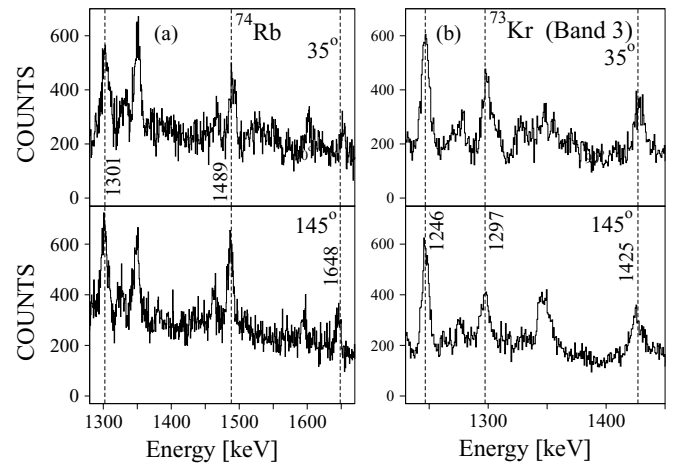


FIG. 2. Partial spectra showing some of the transitions of interest at effective angles of 35° and 145° for band 3 in ^{73}Kr and band 4 in ^{74}Rb . Details of the gates used to create the spectra are given in the text.

transitions (gates on other transitions were not used as they introduced too much contamination into the sum spectrum). This was done for each of the angles described above, and the Doppler-shifted energies were extracted from the summed spectra. A similar procedure was carried out for bands 2 and 3, with gates of 144, 516, and 712 keV being used for band 2 and 744, 892, and 1085 keV for band 3, respectively. For band 4 in ^{74}Rb , the gates used were 304, 478, 520, and 824 keV. Example partial spectra revealing the residual Doppler shifts are shown in Fig. 2 for two of the bands under investigation. The intensities of the 304- and 520-keV γ rays indicate that the order of these two transitions in the $T = 0$ band (band 4) in ^{74}Rb should be reversed from that published by O’Leary *et al.* [23].

Figure 3 shows the results of the total $F(\tau)$ versus spin curves for each of the bands along with the best-fit quadrupole moment curve to the data. The dotted line represents the constant shift ($F_{\text{out}} = 0.891$) for the decays that happen outside the thin target. Because we could obtain spectra only by using gates at the bottom of the bands of interest, feeding was assumed to occur into each state for which lifetimes were extracted. The amount of side-feeding was estimated from the intensities of the observed γ rays and the feeding was assumed to be via a rotational sequence of five transitions with a quadrupole moment equal to that of the in-band decays. Beyond that, the method of analysis used was similar to that quoted in Refs. [11,31]. The decay of the nucleus was modeled using the empirical relation given in Eq. (1) [31].

$$Q_t(I) = Q_t^{\text{top}} + \delta Q_t \sqrt{I^{\text{top}} - I}. \quad (1)$$

The “top” superscript indicates the highest state that was observed experimentally within a given band for which a centroid shift could be measured. From the current data this corresponds to $I^{\text{top}} = 43/2^-, 49/2^-, 45/2^+$ for bands 1, 2, and 3 in ^{73}Kr , respectively, and to 23^+ for the $T = 0$ band in ^{74}Rb . δQ_t represents the variation of the Q_t within a band. The justification for employing the above procedure, rather than using a constant quadrupole moment for the entire band,

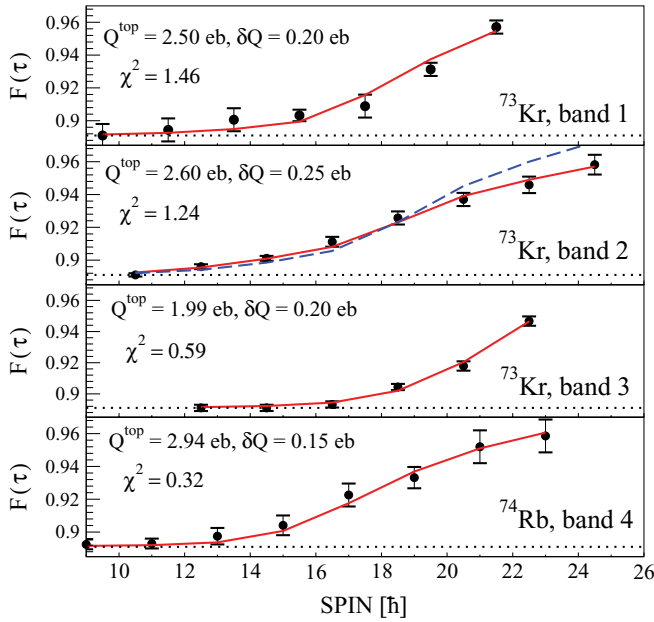


FIG. 3. (Color online) $F(\tau)$ versus spin data for the three bands in ^{73}Kr and band 4 in ^{74}Rb . The dotted line represents the $F(\tau)$ ($=F_{\text{out}}$) value for decays that occur outside of the target. The solid lines show the best fit to the data points using the parameters listed in the figure. The dashed line for band 2 in ^{73}Kr shows the result of the best fit assuming a constant quadrupole moment, Q , of 2.55 eb for the whole band.

can be seen in Fig. 3, panel 2, where band 2 in ^{73}Kr has been fitted assuming a constant Q of 2.55eb. This clearly does not represent the data very well at high spin. Table I summarizes the extracted quadrupole moments for the states in each band studied in ^{73}Kr and ^{74}Rb using the procedure described above.

IV. DISCUSSION

The experimental and theoretical Q_t values are compared in Fig. 4. The calculations were performed earlier using the CNS and CRMF approaches in Refs. [10,23,32]. Pairing was neglected in both calculations. Comparison of the CRMF and cranked relativistic Hartree-Bogoliubov (CRHB) calculations [33] (see Fig. 4 of the current manuscript for ^{74}Rb and Figs. 2 and 11 in Ref. [10] for the results related to the bands in ^{74}Kr and ^{72}Kr) indicates that the impact of pairing on the transition quadrupole moment is less than 0.2 eb at medium and high spins. The standard parametrization of the Nilsson potential [34] was employed in the CNS calculations, whereas the NL3 parametrization of the RMF Lagrangian was used in the CRMF calculations [35]. The calculated configurations are labeled by the number of $g_{9/2}$ protons and neutrons, as $[p, n]$. Furthermore, the configuration assignments for observed bands at high spin in the nuclei of interest is based on Refs. [10,23,32] and are shown in Fig. 5.

The above theoretical approaches have been successfully used to describe the high-spin rotational structures in other nuclei in this mass region [10,11,36,37]. Taking into account that the experimental data are subject to a 10–15% systematic

TABLE I. Level energies, spins, and parities, γ -ray energies, $F(\tau)$ values, and deduced quadrupole moments for rotational bands in ^{73}Kr and ^{74}Rb assuming the functional form of Eq. (1).

E_{level} keV	I_{initial}^{π}	E_{γ} (keV)	$F(\tau)$	Q_t (eb)
^{73}Kr —band 1				
2865	$\frac{19}{2}^{-}$	1034	0.891(7)	2.99(0.08)
4088	$\frac{23}{2}^{-}$	1223	0.894(7)	2.95(0.08)
5408	$\frac{27}{2}^{-}$	1320	0.901(7)	2.90(0.08)
6568	$\frac{31}{2}^{-}$	1160	0.903(4)	2.85(0.08)
7891	$\frac{35}{2}^{-}$	1323	0.909(7)	2.78(0.08)
9401	$\frac{39}{2}^{-}$	1510	0.931(4)	2.70(0.08)
11106	$\frac{43}{2}^{-}$	1705	0.957(4)	2.50(0.08)
^{73}Kr —band 2				
3382	$\frac{21}{2}^{-}$	1097	0.891(1)	3.26(0.08)
4645	$\frac{25}{2}^{-}$	1263	0.896(2)	3.21(0.08)
6027	$\frac{29}{2}^{-}$	1382	0.901(2)	3.16(0.08)
7330	$\frac{33}{2}^{-}$	1303	0.911(3)	3.10(0.08)
8741	$\frac{37}{2}^{-}$	1411	0.926(4)	3.03(0.08)
10356	$\frac{41}{2}^{-}$	1615	0.937(4)	2.95(0.08)
12099	$\frac{45}{2}^{-}$	1743	0.946(5)	2.85(0.08)
13967	$\frac{49}{2}^{-}$	1868	0.958(6)	2.60(0.08)
^{73}Kr —band 3				
4401	$\frac{25}{2}^{+}$	1246	0.891(2)	2.44(0.08)
5615	$\frac{29}{2}^{+}$	1214	0.891(2)	2.39(0.08)
6812	$\frac{33}{2}^{+}$	1197	0.893(2)	2.34(0.08)
8109	$\frac{37}{2}^{+}$	1297	0.904(3)	2.27(0.08)
9534	$\frac{41}{2}^{+}$	1425	0.918(3)	2.19(0.08)
11253	$\frac{45}{2}^{+}$	1719	0.947(3)	1.99(0.08)
^{74}Rb —band 4				
3137	11^{+}	824	0.893(5)	3.31(0.22)
4091	13^{+}	954	0.898(6)	3.28(0.22)
5216	15^{+}	1125	0.904(8)	3.24(0.22)
6517	17^{+}	1301	0.923(9)	3.20(0.22)
8006	19^{+}	1489	0.933(6)	3.15(0.22)
9654	21^{+}	1648	0.952(10)	3.09(0.22)
11411	23^{+}	1757	0.959(10)	2.94(0.22)

error in the absolute value of Q_t (which is not included in the experimental error bars in Fig. 3) because of the uncertainty in the stopping powers, one can say that both the experimentally deduced absolute values of Q_t of the rotational bands in ^{73}Kr and ^{74}Rb and their evolution with spin are in reasonable agreement with the calculations (see Fig. 4).

Because the experimental data on the lifetimes of high-spin bands in $^{73,74}\text{Kr}$ and ^{74}Rb were obtained in the same experiment, the relative transition quadrupole moments between the different bands in these nuclei should not be affected by the uncertainties in the stopping powers, because these uncertainties are the same for all bands. This experimental fact has been used earlier in the confirmation of the additivity principle in

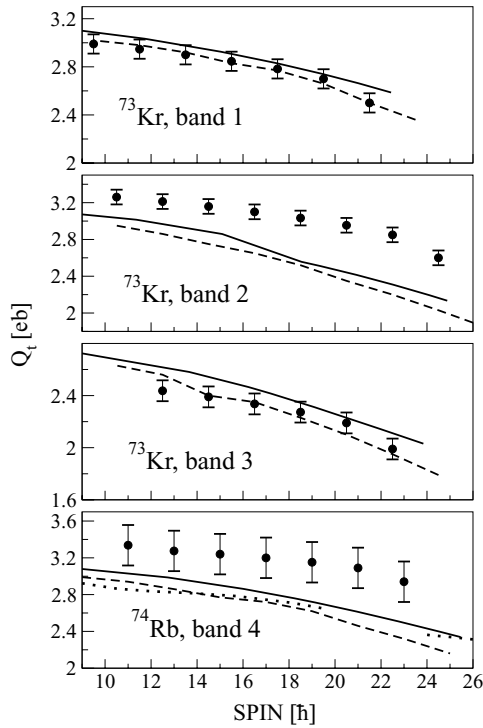


FIG. 4. Comparison of experimental (filled circles) and theoretical Q_t values as a function of spin for bands in ^{73}Kr and ^{74}Rb . Solid and dashed lines show results for CRMF and CNS calculations, respectively. The bottom panel also shows results of CRHB calculations at both low and high spin (dotted lines).

the study of quadrupole moments of superdeformed bands in the $A \sim 150$ [15,17–19] and $A \sim 130$ [20,21] mass regions for nuclei that are predominantly characterized by axially symmetric near-prolate deformation. The data for the $^{73,74}\text{Kr}$ and ^{74}Rb nuclei allow, for the first time, a similar test of the additivity principle for transition quadrupole moments in rotational bands that are not axially prolate but are expected to possess some degree of γ deformation [10].

Figure 6 shows relative transition quadrupole moments between the bands that differ by the occupation of one single-particle orbital (see Fig. 5). The pairs of bands $^{74}\text{Kr}(\text{A})$ - $^{73}\text{Kr}(1)$, $^{74}\text{Kr}(\text{B})$ - $^{73}\text{Kr}(2)$, and $^{74}\text{Kr}(\text{GSB})$ - $^{73}\text{Kr}(3)$ differ from each other by the occupation of one $\nu g_{9/2}(\alpha = -1/2)$ orbital. It is expected that the relative transition quadrupole moments of these bands will be approximately the same if the additivity principle for transition quadrupole moments holds [15]. This feature is seen in the CNS and CRMF calculations where the ΔQ_t values associated with the occupation of the $\nu g_{9/2}(\alpha = -1/2)$ orbital are around 0.2eb and do not show appreciable dependence on the pairs of bands compared [see Figs. 6(a)–6(c)]. Experimentally, the relative ΔQ_t values of the pairs of bands, which differ in the occupation of the $\nu g_{9/2}(\alpha = -1/2)$ orbital, show appreciable scattering from pair to pair and only in the case of the $^{74}\text{Kr}(\text{GSB})$ - $^{73}\text{Kr}(3)$ pair [see Fig. 6(c)] are they close to theoretical predictions. The relative ΔQ_t values of the other two pairs [see Figs. 5(a) and 5(b)] deviate from the calculations by 0.2 – 0.4eb and, in one case, even differ by the sign. In the $A \sim 150$ nuclei the additivity principle

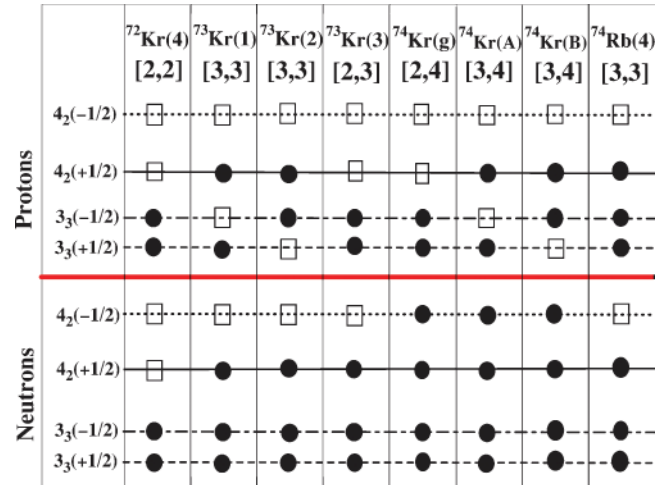


FIG. 5. (Color online) Configuration assignments to high-spin bands of $^{72,73,74}\text{Kr}$ and ^{74}Rb . Solid circles and open squares are used to indicate occupied and unoccupied orbitals, respectively. The orbitals are labeled with the main oscillator quantum, N , the signature α (in parantheses) and as a subscript the position of the orbitals within the N shell (for $N = 4$ states) and within the group of low- j orbitals for the $N = 3$ shell. The orbitals below and above the depicted orbitals are occupied and empty, respectively.

for quadrupole moments is fulfilled with somewhat better precision [17,18,38] than in the current case.

In a similar way, the pairs of bands $^{74}\text{Rb}(4)$ - $^{73}\text{Kr}(1)$, $^{74}\text{Rb}(4)$ - $^{73}\text{Kr}(2)$, and $^{74}\text{Rb}(4)$ - $^{73}\text{Kr}(3)$ differ in the occupation of the $\pi 3_3(\alpha = -1/2)$, $\pi 3_3(\alpha = +1/2)$, and $\pi g_{9/2}(\alpha = +1/2)$ orbitals, respectively (see Fig. 5). Figure 6 once again shows that there is no consistent agreement between calculations and experiment, and that the discrepancy between experiment and theory can reach 0.4eb (representing almost 15% of total transition quadrupole moment); a similar value to that seen between the pairs of bands differing by the $\nu g_{9/2}(\alpha = -1/2)$ orbital. Thus, the present experimental results suggest that the additivity principle for the transition quadrupole

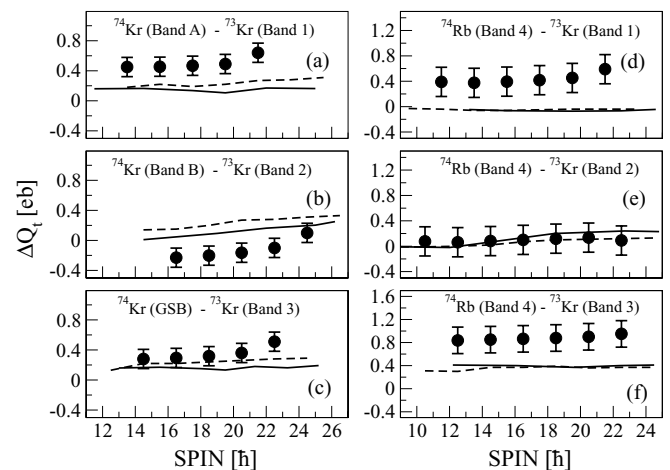


FIG. 6. Relative transition quadrupole moments ΔQ_t as a function of spin. The band in the lighter nucleus is used as a reference so the ΔQ_t measures the effect of the additional particle.

moments is violated in triaxially deformed rotational bands of the $A \sim 70$ mass region.

Clearly one would wish to investigate the possible reasons for such a violation of the additivity principle for transition quadrupole moments. Unfortunately, the measurements of the Q_t values in ^{73}Kr and ^{74}Rb do not extend up to the highest observed spins where the unpaired picture is fully justified: the present measurements mainly cover the spin range where some pairing may be present. We note, however, that calculations without pairing can describe reasonably well both the alignment and the level energy minus a rigid rotor reference energy, $E - E_{\text{RLD}}$, curves at spin $I \geq 15\hbar$ (see Refs. [23,32]). This information, together with the above discussed comparison of the CRMF and CRHB Q_t values, suggests that the like-particle pairing is of relatively minor importance and therefore should not have a major impact on the Q_t values.

An interesting question is whether the isoscalar $t = 0$ neutron-proton pairing is involved in this violation of the additivity principle. The negative-parity bands 1 and 2 in ^{73}Kr are primary suspects in that respect because they have unusual band crossings taking place at $\omega \sim 0.64$ MeV/ \hbar [32]. These crossings were tentatively assigned as being due to a change from the one-quasiparticle (1-qp) $[\nu(pf)]$ configuration to the 3-qp $[\pi(pf)g_{9/2} \otimes \nu(g_{9/2})]$ configuration rather than the expected 1-qp $[\nu(pf)]$ to the 5-qp $[\pi(g_{9/2})^2 \otimes \nu(pf)(g_{9/2})^2]$ configuration, which involves the simultaneous alignment of $g_{9/2}$ proton and neutron pairs. An additional and more gradual crossing takes place within these bands at $\omega \sim 0.9$ MeV/ \hbar . The CNS and CRMF calculations suggest that after this crossing the negative-parity bands are well described in the formalism without pairing by the [3,3] configurations (this crossing is even present in the CNS calculations for the [3,3] conf. (see Fig. 7 in Ref. [32]), which suggests that it is not necessarily due to pairing).

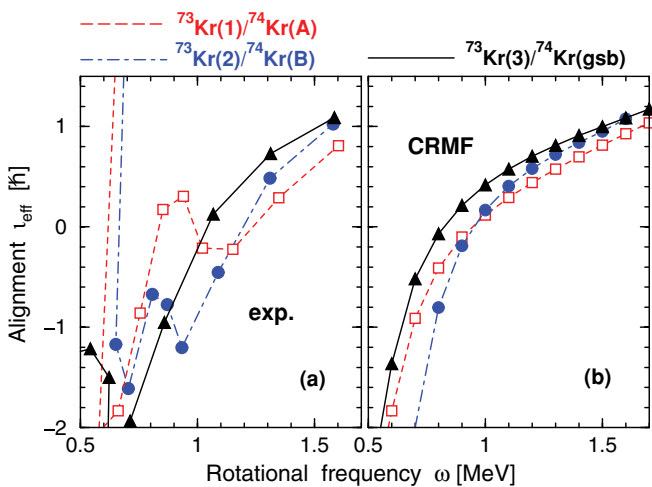


FIG. 7. (Color online) (a) Experimental and (b) calculated effective alignments of the bands (configurations) that differ in the occupation of the $\nu g_{9/2}(\alpha = -1/2)$ orbital. The same combination of the symbols and lines is used for experimental values (left panel) and their theoretical counterparts (right panel).

It was speculated in Ref. [32] and later elaborated in Ref. [39] that this transition from 1-qp to 3-qp configurations involves $t = 0 np$ pair scattering, thus providing an explanation as to why the $E2$ transitions between these configurations are not hindered. However, this interpretation has been questioned in Ref. [10] by considering related structures in ^{70}Br and ^{72}Kr . Moreover, the alignment features of these bands in ^{73}Kr are well described in the total Routhian surface (TRS) formalism with only $t = 1$ like-particle pairing (cf. Fig. 8 in Ref. [32] with Fig. 4 in Ref. [39]); although contrary to experiment the band crossing at $\omega \sim 0.9$ MeV/ \hbar is washed out in the calculations involving $t = 0 np$ pairing. In addition, it turns out that similar bands in ^{75}Rb can be well described without involving $t = 0 np$ pairing [39]. Thus, from our current understanding of the situation it is quite unlikely that the violation of the additivity principle can be associated with isoscalar $t = 0$ neutron-proton pairing.

Additional insight into the additivity of physical observables is provided by the analysis of the effective (relative) alignments i_{eff} of pairs of bands that differ in the occupation of the same orbital, in our case, of the $\nu g_{9/2}(\alpha = -1/2)$ orbital (see Fig. 7). The effective alignment $i_{\text{eff}}^{B,A}$ of the two bands A and B is defined [40] as the difference in their spins at the same rotational frequency ω : $i_{\text{eff}}^{A,B}(\omega) = I_B(\omega) - I_A(\omega)$. It depends on the alignment properties of the single-particle orbital(s) by which the two bands differ and on the polarization effects induced by the particle(s) in these orbital(s). It is expected that the effective alignments of different pairs of bands will be approximately the same if the additivity principle for angular momentum alignments holds [16]. Indeed, in the CRMF calculations these alignments are close to each other within approximately $0.3\hbar$ [see Fig. 7(b)] at frequencies larger than 1.0 MeV/ \hbar . Clearly, the scattering of experimental i_{eff} values is larger in the same frequency range [see Fig. 7(a)]. This indicates that the angular momenta are less additive experimentally than the calculations suggest. This in turn suggests that some correlations that act to destroy the additivity principle are missing in model calculations. However, these correlations are unlikely to be associated with np pairing, because a similar large scattering of effective alignments attributable to the same orbitals has been seen before in the smooth terminating bands of the $A \sim 110$ mass region in the spin range where the nuclei are triaxial (see Ref. [40]). In these latter bands the np pairing plays no role.

A possible scenario for the band crossing observed at $\omega \sim 0.9$ MeV/ \hbar in the negative-parity bands 1 and 2 in ^{73}Kr , which is visible in the effective alignment plots shown in Fig. 7(a), and the structure of these bands in the $\omega = 0.62$ – 0.9 MeV/ \hbar frequency range, can be suggested from the analysis of the configurations involved and the relevant single-particle Routhians. The structure of the single-particle 3_3 orbital in which the hole is created (see Fig. 5) is different at $\omega \sim 0.64$ – 0.9 MeV/ \hbar (emerging from the [310]1/2 Nilsson state) and at $\omega \geq 0.9$ MeV/ \hbar (emerging from the [312]3/2 Nilsson state), leading to an observed crossing. This also suggests that at medium spin, corresponding to the frequencies $\omega = 0.64$ – 0.9 MeV/ \hbar , the configurations of the observed bands in terms of occupation of high- j intruder orbitals are the same as at high spin.

The following facts support this interpretation. First, the band crossing at $\omega \sim 0.9$ MeV/ \hbar is not seen in the $^{73}\text{Kr}(3)/^{74}\text{Kr}(\text{gsb})$ pair; the $3_3(\pm 1/2)$ orbitals are occupied in both these bands. Thus, the i_{eff} curve for this pair is due to the alignment of the single $\nu g_{9/2}(\alpha = -1/2)$ orbital. On the contrary, this crossing is seen in the $^{73}\text{Kr}(1)/^{74}\text{Kr}(\text{A})$ and $^{73}\text{Kr}(2)/^{74}\text{Kr}(\text{B})$ pairs, the $3_3(\alpha = -1/2)$ and $3_3(\alpha = +1/2)$ orbitals are not occupied in the bands forming the first and second pairs, respectively (see Fig. 5). The effective alignments of these pairs of bands reflect the alignment of the single $\nu g_{9/2}(\alpha = -1/2)$ orbital at $\omega \geq 0.9$ MeV/ \hbar . However, at frequencies $\sim 0.64\text{--}0.9$ MeV/ \hbar , they are shifted up by approximately $1\hbar$ compared with the expected alignment of the single $\nu g_{9/2}(\alpha = -1/2)$ orbital [which is similar to that observed in the $^{73}\text{Kr}(3)/^{74}\text{Kr}(\text{gsb})$ pair]. This difference is due to the fact that the compared bands in this frequency range differ by the alignment of two additional low- j $N = 3$ orbitals.

For that scenario to hold, it is necessary that this crossing is active in the $^{73}\text{Kr}(1,2)$ bands but not present in the $^{74}\text{Kr}(\text{A,B})$ bands. In the calculations, the deformations of the $^{74}\text{Kr}(\text{A,B})$ bands are larger than those for bands 1 and 2 in ^{73}Kr . This increase in deformation is due to the presence of an additional $g_{9/2}$ neutron. The crossing of the $[310]1/2$ and $[312]3/2$ orbitals takes place at lower frequency with increasing deformation. If the deformation of the $^{74}\text{Kr}(\text{A,B})$ bands is sufficiently large, the crossing of the above mentioned orbitals will occur below the experimentally observed lower frequency range in these bands. The detailed theoretical description of this process requires very accurate reproduction of the single-particle energies for the participating $N = 3$ orbitals; this is not achievable without additional optimization of the Nilsson potential or the RMF Lagrangian.

The absence of the holes in the 3_3 orbitals in the structure of the $^{74,75}\text{Rb}$ bands provides a possible explanation as to why

they are well described within the standard models containing only like-particle pairing [23,39]. This is contrary to the case of the negative-parity bands in ^{73}Kr that most likely requires a very precise description of the single-particle energies of the 3_2 and 3_3 orbitals.

V. SUMMARY

In summary, lifetimes have been obtained for high-spin rotational bands of ^{73}Kr and ^{74}Rb . These have allowed transition quadrupole moments to be deduced. Relative transition quadrupole moments were studied for the first time both as a function of spin and for triaxial shapes. The data indicate that the additivity of transition quadrupole moments is violated. This is contrary to theoretical results that show that even for triaxial shapes the additivity of transition quadrupole moments is reasonably well fulfilled. The nature of this contradiction is not fully understood, although it is not excluded that important correlations are missing in the models.

ACKNOWLEDGMENTS

This research was partially supported by the Natural Science and Engineering Research Council of Canada, the U.K. Engineering and Physical Sciences Research Council, and the U.S. Department of Energy under Contract Nos. DE-FG02-07ER41459, DE-FG-07ER41459, DE-AC02-06CH11357, and DE-FG02-88ER40406. CA acknowledges the support offered by the Swedish Research Council for Higher Education and Research and the Swedish Research Council.

-
- [1] B. S. Nara Singh *et al.*, Phys. Rev. C **75**, 061301(R) (2007).
 - [2] E. Clement *et al.*, Phys. Rev. C **75**, 054313 (2007).
 - [3] W. Nazarewicz *et al.*, Nucl. Phys. **A435**, 397 (1985).
 - [4] B. J. Varley *et al.*, Phys. Lett. **B194**, 463 (1987).
 - [5] G. de Angelis *et al.*, Phys. Lett. **B415**, 217 (1997).
 - [6] E. Bouchez *et al.*, Phys. Rev. Lett. **90**, 082502 (2003).
 - [7] D. Rudolph *et al.*, Phys. Rev. C **56**, 98 (1997).
 - [8] C. Chandler *et al.*, Phys. Rev. C **56**, R2924 (1997).
 - [9] F. Becker *et al.*, Eur. Phys. J. A **4**, 103 (1999).
 - [10] A. V. Afanasjev and S. Frauendorf, Phys. Rev. C **71**, 064318 (2005).
 - [11] J. J. Valiente-Dobón *et al.*, Phys. Rev. Lett. **95**, 232501 (2005).
 - [12] C. E. Svensson *et al.*, Phys. Rev. Lett. **80**, 2558 (1998).
 - [13] R. Wadsworth *et al.*, Phys. Rev. Lett. **80**, 1174 (1998).
 - [14] G. de France, C. Baktash, B. Haas, and W. Nazarewicz, Phys. Rev. C **53**, R1070 (1996).
 - [15] W. Satula, J. Dobaczewski, J. Dudek, and W. Nazarewicz, Phys. Rev. Lett. **77**, 5182 (1996).
 - [16] M. Matev, A. V. Afanasjev, J. Dobaczewski, G. A. Lalazissis, and W. Nazarewicz, Phys. Rev. C **76**, 034304 (2007).
 - [17] G. Hackman, R. V. F. Janssens, E. F. Moore, D. Nisius, I. Ahmad, M. P. Carpenter, S. M. Fischer, T. L. Khoo, T. Lauritsen, and P. Reiter, Phys. Lett. **B416**, 268 (1998).
 - [18] S. T. Clark *et al.*, Phys. Rev. Lett. **87**, 172503 (2001).
 - [19] L. B. Karlsson, I. Ragnarsson, and S. Aberg, Nucl. Phys. **A639**, 654 (1998).
 - [20] R. W. Laird *et al.*, Phys. Rev. Lett. **88**, 152501 (2002).
 - [21] M. A. Riley *et al.*, Acta Phys. Pol. B **32**, 2683 (2001).
 - [22] B. Cederwall *et al.*, Nucl. Instrum. Methods A **354**, 591 (1995).
 - [23] C. D. O'Leary *et al.*, Phys. Rev. C **67**, 021301(R) (2003).
 - [24] A. V. Afanasjev, D. B. Fossan, G. J. Lane, and I. Ragnarsson, Phys. Rep. **322**, 1 (1999).
 - [25] A. V. Afanasjev, J. König, and P. Ring, Nucl. Phys. **A608**, 107 (1996).
 - [26] I. -Y Lee, Nucl. Phys. **A520**, 641c (1990).
 - [27] D. G. Sarantites *et al.*, Nucl. Instrum. Methods A **383**, 506 (1996).
 - [28] F. Lerma *et al.*, Phys. Rev. C **67**, 044310 (2003).
 - [29] D. Seweryniak *et al.*, Nucl. Instrum. Methods A **340**, 353 (1994).
 - [30] C. E. Svensson *et al.*, Nucl. Instrum. Methods A **396**, 288 (1997).
 - [31] J. J. Valiente-Dobón *et al.*, Phys. Rev. C **71**, 034311 (2005).
 - [32] N. Kelsall *et al.*, Phys. Rev. C **65**, 044331 (2002).
 - [33] A. V. Afanasjev, P. Ring, and J. König, Nucl. Phys. **A676**, 196 (2000).
 - [34] T. Bengtsson and I. Ragnarsson, Nucl. Phys. **A436**, 14 (1985).

- [35] G. A. Lalazissis, J. König, and P. Ring, Phys. Rev. C **55**, 540 (1997).
- [36] C. Andreoiu *et al.*, Phys. Rev. C **75**, 041301(R) (2007).
- [37] A. V. Afanasjev, I. Ragnarsson, and P. Ring, Phys. Rev. C **59**, 3166 (1999).
- [38] D. Nisius *et al.*, Phys. Lett. **B392**, 18 (1997).
- [39] R. A. Wyss, P. J. Davies, W. Satula, and R. Wadsworth, Phys. Rev. C **76**, 011301(R) (2007).
- [40] A. V. Afanasjev and I. Ragnarsson, Nucl. Phys. **A628**, 580 (1998).